Combined ARPES and STM study of Pb/Au(111) Moiré structure: One overlayer, two symmetries

A. Crepaldi,[1,*] S. Pons,[1,2] E. Frantzeskakis,[3] F. Calleja,[1] M. Etzkorn,[1] A. P. Seitsonen,[4] K. Kern,[1,5] H. Brune,[1] and M. Grioni[1]

[1]*Institut de Physique de la Matière Condensée (ICPM), Ecole Polytechnique Fédérale de Lausanne (EPFL), Station 3, CH-1005 Lausanne, Switzerland*

[2]*Institut des NanoSciences de Paris (INSP), Université Pierre et Marie Curie (UPMC) - Paris 6, CNRS UMR 7588, France*

[3]*Synchrotron SOLEIL, L'Orme des Merisiers, Saint Aubin-BP 48, 91192 Gif sur Yvette Cedex, France*

[4]*Physikalisch-Chemisches Institut, University of Zürich, CH-8057 Zürich, Switzerland*

[5]*Max-Plank-Institut für Festkörperforschung, D-70569, Stuttgart, Germany*

(Received 15 February 2013; revised manuscript received 11 March 2013; published 27 March 2013)

The structural and electronic properties of a Pb monolayer (ML) grown on Au(111) are investigated by scanning tunneling microscopy (STM) and angle resolved photoelectron spectroscopy (ARPES). We find an incommensurate Moiré structure with an approximate (5.77 × 5.77) R21.5° unit cell, and two rotational domains. We observe three Pb-derived bands of p orbital character. The symmetry properties and sharpness of their Fermi surfaces are remarkably different. They reflect the different degrees of hybridization of these bands with the Au(111) bulk continuum.

DOI: 10.1103/PhysRevB.87.115138 PACS number(s): 73.20.At, 79.60.−i

I. INTRODUCTION

Angle resolved photoelectron spectroscopy (ARPES) is ideally suited to probe the influence of commensurate and incommensurate charge (spin) modulations on the electronic structure of solids.[1–3] Characteristic signatures of superperiodicities have been observed by ARPES in bulk materials[4–6] and at ordered interfaces.[7–16] Lead overlayers on both metallic and semiconducting substrates are especially interesting in this respect. It is found that, due to their high lateral stiffness, monolayers (ML) of Pb form dense Moiré superstructures. The corrugation of the overlayer reduces the bonding strength to the substrate[17] and contributes to the remakable surfactant effect of Pb observed, e.g., in the homoepitaxial growth of Cu(111).[18,19] ARPES was exploited to determine the band structure and the electron coherence length of a melting Pb layer on Cu(111).[20] The unexpected observation of superconductivity in the 4/3 ML dense phase of Pb on Si(111)[21,22] has further stimulated the interest for Pb-based interfaces.

Here we report scanning tunneling microscopy (STM) and low-energy electron diffraction (LEED) data revealing a two-domain incommensurate Moiré structure for a Pb ML on Au(111). ARPES identifies three interface bands: two of them have (mainly) Pb p_{xy} character while the third one has Pb p_z character. The behavior of the two Pb p_{xy} states is remarkably different: one adjusts to the symmetry of the Au(111) substrate, whereas the other displays the symmetry of the two-domain modulated overlayer. The p_z state is strongly broadened in energy and momentum, similar to previous observations for Pb MLs on Ag(111)[7] and on Cu(111).[18] These differences reflect the orbital-dependent hybridization of the three interface states with the continuum of substrate bulk states.

II. EXPERIMENT

The Au(111) substrate was cleaned by repeated sputtering (with Ar^+ at 300 K, 1 keV for 30 minutes) and annealing (800 K for 25 minutes) cycles. In the ARPES experiments, the sharpness of the LEED pattern and of the spin-split Shockley surface state were used as indicators of the order and cleanliness of the surface. Pb was evaporated on the substrate at 300 K (room temperature or RT) from a calibrated EFM3 Omicron evaporator, at a rate of 0.3 ML/min. The structural quality of the interface, monitored by LEED, improved after a short post-annealing at 400 K. ARPES mesurements were performed at RT with a Specs Phoibos 150 hemispherical analyzer. The experimental energy resolution was set to 10 meV. The UV light source was a monochromatized high-brightness Gammadata VUV 5000 lamp operating at the He Iα (21.22 eV) line. Further ARPES measurements at liquid nitrogen temperature (not shown) indicate that no modification of the electronic properties of the interface occurs when varying the temperature in this range. STM experiments were performed in a separated UHV system equipped with a home-built 0.4 K STM. In the measurements presented here the sample temperature was 4 K, and the indicated bias voltage refers to the sample potential.

III. RESULTS

Large-scale STM images reveal that the Pb monolayer is ordered over large terraces. The constant-current STM image of Fig. 1(a) displays atomic resolution together with a long-range modulation, indicative of a Moiré structure. The periodicity of the overlayer is best determined from the Fourier transform map of Fig. 1(b), obtained from a larger (20 × 20 nm^2) STM image. It exhibits the hexagonal pattern of the Pb ML (red circles), and the corresponding in-plane Pb-Pb distance is essentially identical to the Pb bulk value of 3.50 Å. Additional spots associated with the Moiré structure define a hexagonal pattern (black circles) which is 4.74 times smaller than the Pb pattern, and rotated by $\beta = 26.5° \pm 1°$. Complementary information is obtained from LEED which, unlike STM, also probes the underlying Au(111) substrate. Indeed, the most intense spots in the LEED pattern of Fig. 1(c) are the first-order diffraction spots of the Au substrate (green hexagon). Two smaller, identical patterns (blue and red hexagons) rotated by ±5°, whose size corresponds to

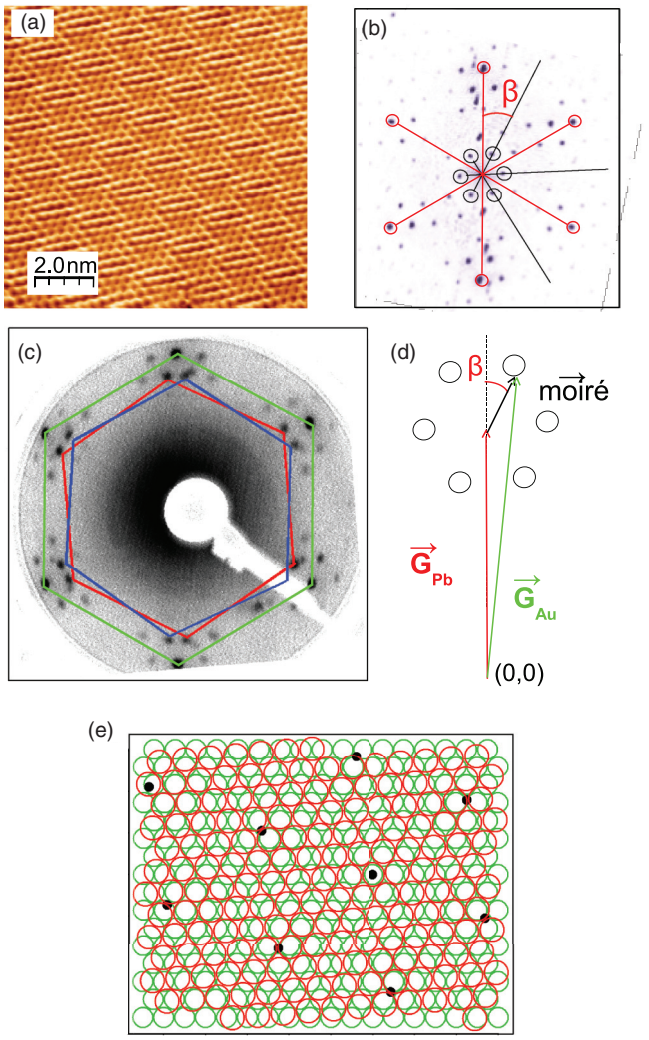

FIG. 1. (Color online) (a) Constant-current STM image of 1 ML Pb on Au(111), showing one rotational domain of the Moiré structure ($V_t = 2.0$ V and $I_t = 0.14$ nA, $T = 4.2$ K). (b) The Fourier transform of a larger (20×20 nm^2) STM image exhibits the hexagonal pattern (red circles) of a Pb ML and satellites corresponding to the Moiré superstructure spots (black circles). (c) LEED image showing the Au(111) (green) and two equivalent Pb (blue and red) hexagonal patterns, and Moiré satellites. (d) Reciprocal lattice vectors of the Au, Pb (one domain), and Moiré patterns. (e) In-plane structural model of the interface (one domain). Au (Pb) atoms are represented by green (red) circles.

the periodicity of the Pb ML, can be identified inside the Au hexagon. Clearly, two equivalent rotational domains are simultaneously present in the Pb overlayer. Higher order diffraction spots show the good crystalline quality of the samples studied by ARPES. The relation between the substrate and overlayer periodicities, as determined from STM[23] and LEED, is best seen by the reciprocal lattice vectors shown in Fig. 1(d). The Moiré unit cell is approximately given by (5.77×5.77) R21.5° with respect to the Au(111) substrate. It is compatible with a rotation of ±5° between the Pb and the Au(111) lattices;[24] see the ball model in Fig. 1(e). The good agreement between the low-temperature (4 K) STM data and the room-temperature LEED data indicates

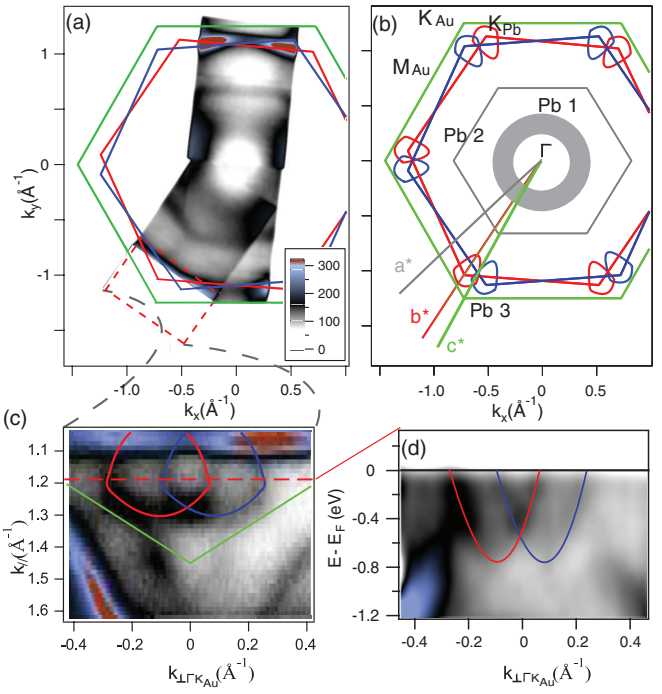

FIG. 2. (Color online) (a) ARPES Fermi surface (FS) map. Hexagons outline the Au(111) surface BZ (green) and the BZs of the two Pb domains (red and blue). The FS sheets of the three Pb-derived bands are schematically illustrated in (b). (c) Closeup of the area within the dashed rectangle in (b); red and blue lines outline the Pb3-derived pockets for the two Pb domains. (d) E vs k dispersion of Pb3 (two domains) along the dashed line in (c), perpendicular to $\overline{\Gamma K}_{Au}$.

that, despite the strong electron-phonon coupling of Pb, the structure of this interface does not vary in this temperature range.

We now turn to the ARPES data, and to the experimental band structure arising from the interaction of the Pb ML with the substrate. Figure 2(a) shows a portion of the Fermi surface (FS), extracted from ARPES measurements along the $\overline{\Gamma K}$ and two inequivalent $\overline{\Gamma M}$ high symmetry directions. The green hexagon is the Au(111) surface Brillouin zone (BZ); the smaller red and blue hexagons define the Brillouin zones of a Pb monolayer rotated by ±5°. The most intense feature, near the Au BZ boundary, originates from the bulk Au sp valence band. All the remaining features are Pb derived, and are schematically represented in Fig. 2(b). Previous tight-binding calculations performed for dense Pb monolayers on Cu(111) and Ag(111),[7,18,20] found three Pb-derived bands: a band with p_z orbital character with the smallest Fermi wave vector, hereafter labeled Pb1, and two bands with p_{xy} character, labeled Pb2 and Pb3. The same picture is also consistent with our data, namely with the multisheet Fermi surface of Fig. 2(a). The diffuse, almost circular contour around the $\overline{\Gamma}$ point is attributed to Pb1, by analogy with the Cu(111) and Ag(111) cases. Pb2 forms a larger hexagonal Fermi surface. This single hexagonal contour is aligned with the BZ of the substrate. The symmetry of the FS associated with the third band is remarkably different. Pb3 crosses the Fermi level (E_F) near the corners of the Pb BZ, as illustrated in panel (c),

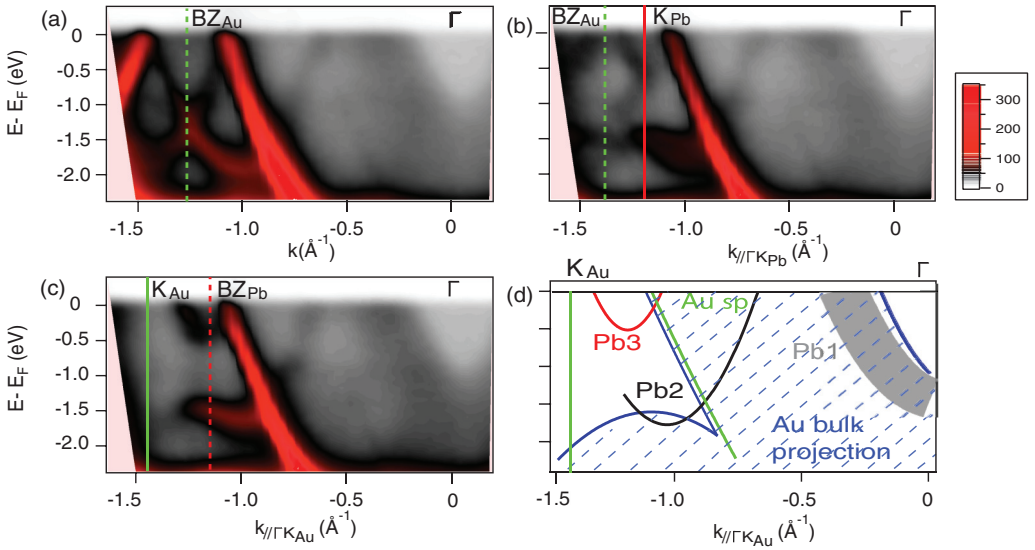

FIG. 3. (Color online) ARPES band dispersion along (a) a line 15° from $\overline{\Gamma K}_{Au}$ [line a* in Fig. 2(b)]; (b) $\overline{\Gamma K}_{Pb}$ [line b* in Fig. 2(b)]; and (c) $\overline{\Gamma K}_{Au}$ [line c* in Fig. 2(b)]. Vertical lines (solid lines for high-symmetry points) indicate the BZ boundaries. The experimental dispersion (c) is schematically illustrated in (d), where the calculated Au band structure projected on the (111) surface from Ref. 25 is also shown.

which shows a closeup of the area within the dashed rectangle in Fig. 2(a). It forms a trigonally distorted pocket around the corners ($\overline{K}_{Pb}$) of the BZ of *both* Pb rotational domains. The adjacent pockets partially overlap with each other, and also with the substrate FS, the strongest feature in panel (c). Figure 2(d) illustrates the nearly parabolic E vs k dispersion of the overlapping Pb3 electron pockets along the dashed line in panel (c), perpendicular to the $\overline{\Gamma K}_{Au}$ direction.

Figure 3 presents the experimental band structure over a broad momentum range, along the three lines marked a*, b*, c* in Fig. 2(b). They correspond to (a) a line 15° from $\overline{\Gamma K}_{Au}$, (b) the $\overline{\Gamma K}_{Pb}$ direction for one domain, and (c) the $\overline{\Gamma K}_{Au}$ direction ($\overline{\Gamma K}_{Au} = 1.45$ Å^{-1}; $\overline{\Gamma K}_{Pb} = 1.19$ Å^{-1}). A sketch of the experimental ARPES dispersion along $\overline{\Gamma K}_{Au}$ is shown in panel (d), which also includes the projection of the calculated Au bulk band structure onto the (111) surface.[25] Two of the Pb-derived bands (Pb1 and Pb2) and the dominant signal from the Au sp band, are visible in panel (a). Pb1, which disperses upward from $\overline{\Gamma}$, lies entirely within the continuum of the Au bulk states. The bottom of this band around −1.5 eV and its Fermi level crossing near $k_{F1} = -0.35$ Å^{-1} are poorly defined, because its spectral weight is diffuse both in energy and momentum, similar to the case of Pb/Ag(111),[7] and consistent with the blurred circular FS contour of Fig. 2. Pb2 exhibits a nearly parabolic upward dispersion from its minimum at $k_{\parallel} = 1$ Å^{-1} and −1.9 eV. Its intensity is strongly reduced after crossing the Au sp band and entering the projected bulk continuum. The Fermi level crossing at $k_{\parallel} \sim -0.6$ Å^{-1} is part of the single hexagonal contour of Fig. 2(b). Folding of Pb2 and of the Au sp band around the Au BZ boundary generates clear replicas of these bands. The Pb3 band is visible near K_{Pb} along lines b* [panel (b)] and c* [panel (c)] which intersect the electron pockets. The dispersion of Pb2 is strongly modified with respect to panel (a) beyond the Pb BZ boundary. A gap opens between Pb2 and Pb3, indicating an interaction between the two bands.

Neither the FS of Fig. 2 nor the bands of Fig. 3 exhibit replicas with the periodicity of the Moiré structure. This contrasts, e.g., with recent observations for graphene on a metallic substrate,[15,16] where the Moiré structure gives rise to folded bands, with intensities proportional to the strength of the superlattice potential.[7,18] Therefore, we conclude that the Moiré potential has a comparatively smaller amplitude in the present case.

IV. DISCUSSION

The interaction between the Pb overlayer and the Au(111) substrate, and their different periodicities, are at the origin of a nontrivial band structure. We have performed a model tight-binding (TB) calculation as a guide to the interpretation of the ARPES results, namely to gain insight on the origin of the gap between the Pb2 and Pb3 bands observed in Fig. 3. As a first step, we model a free-standing Pb overlayer by a two-dimensional hexagonal lattice, with three p orbitals per site. The p_x and p_y orbitals couple in-plane to nearest neighbors via directional cosines, and give rise to two hybrid p_{xy} bands, which are orthogonal to the p_z band due to $+z/-z$ inversion symmetry. Model parameters quantify the Slater-Koster overlap integral[26] (see Appendix). The only free parameter is $(pp\pi/pp\sigma)$. Similar oversimplified models have already been used to analyze the electronic structure of the Pb/Ag(111) and Pb/Cu(111) interfaces.[7,18] The band structure shown in Fig. 4(a) reproduces the results of the previous studies. In particular, as expected, there is no interaction gap between the p_{xy} and p_z states and, at variance with experiment, between the two p_{xy} states at the $\overline{K}$ point.

A possible source of hybridization between the Pb bands is via the interaction with the substrate, which breaks the $+z/-z$ inversion symmetry. This interaction may be driven by the buckling of the Pb layer, as already proposed for the Pb/Cu(111) interface.[18] Following Ref. 27 we have modeled

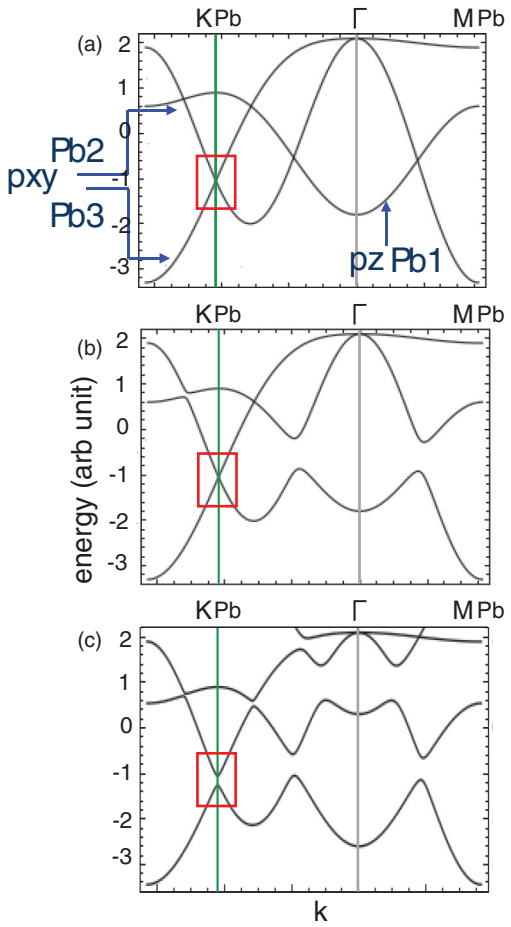

FIG. 4. (Color online) (a) Calculated TB bands for p states on a free-standing hexagonal Pb monolayer. Two bands (p_{xy}) have hybrid p_x and p_y orbital character; the third has p_z character. (b) A gap opens between the p_{xy} and p_z states if the $+z/-z$ symmetry is broken. (c) The degeneracy of the two p_{xy} states at $\overline{\mathrm{K}}$ is lifted when the sixfold in-plane symmetry is also broken by the interaction with the substrate. The parameters of the TB model are summarized in the Appendix.

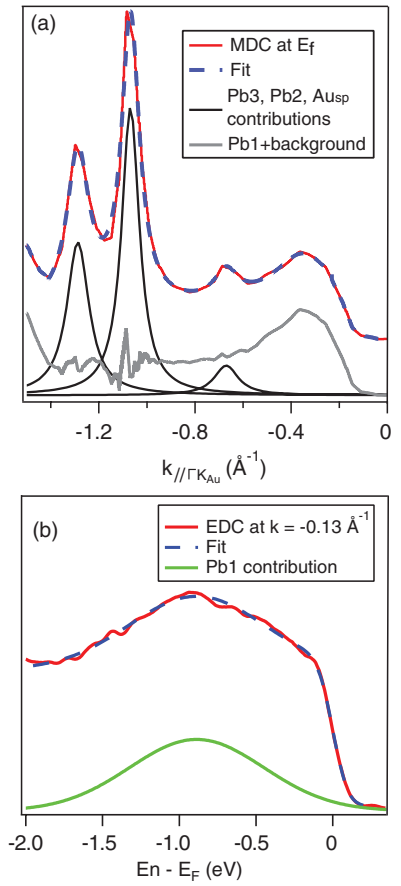

FIG. 5. (Color online) (a) Momentum distribution curve (MDC) at E_F along $\overline{\Gamma\mathrm{K}}_{\mathrm{Au}}$. The widths (FWHM) of the Lorentzian peaks used in the fit are 0.11 Å^{-1} (Pb2), 0.11 Å^{-1} (Pb3), and sp 0.08 Å^{-1} (Au sp). The fit residual (grey) describes the remaining Pb1 peak and the background related to the Au bulk continuum. (b) The energy distribution curve (EDC) corresponding to $k = -0.13$ Å^{-1}. A Gaussian fit of the Pb1 state yields $\Delta E = 1.1 \pm 0.1$ eV (FWHM).

in Fig. 4(b) the presence of the substrate by introducing an asymmetry in the p_z state. The p_{xy} and p_z bands now hybridize, and gaps appear in correspondence of the avoided crossings. Nevertheless, the p_{xy} states remain degenerate at $\overline{\mathrm{K}}$. The degeneracy is a necessary consequence of the artificial sixfold symmetry of the free-standing ML, which is broken by explicitly introducing an interaction with the substrate. We have extended the TB model to include an interaction between the Pb p orbitals and an s orbital of the substrate, with three substrate atoms placed in *hollow* sites around each Pb atom. Figure 4(c) shows that in this case a gap, proportional to the sp hybridization, opens between the p_{xy} states at the $\overline{\mathrm{K}}$ point, as observed by ARPES. Moreover, the interaction with the substrate naturally breaks the $+z/-z$ inversion symmetry, and therefore opens a hybridization gap between the p_{xy} and p_z states, without any *ad hoc* asymmetry parameter. Such a gap was previously reported for Pb/Cu(111).[18] It cannot be experimentally observed here, because the (avoided) crossing of the two bands lies above the Fermi level.

The diffuse spectral weight distribution of the Pb1 band is a distinctive and unusual feature of the ARPES data of Fig. 3. This aspect is further illustrated in Fig. 5. Figure 5(a) shows a momentum distribution curve (MDC) extracted at E_F, along the $\overline{\Gamma\mathrm{K}}_{\mathrm{Au}}$ direction. The peaks corresponding to the Pb2, Pb3, and the Au sp bands were fitted by Lorentzians. The fit residual (grey) describes the remaining Pb1 band and the background related to the Au bulk continuum. This background reflects indirect transitions, and is proportional to the integrated density of states along k_z.[28] Remarkably, the momentum width of the Pb1 peak is 4–5 times broader than those of the other band features. Figure 5(b) gives a complementary view along the energy axis. It shows an energy distribution curve (EDC) corresponding to a wave vector $k = -0.13$ Å^{-1}, where the Pb1 contribution is dominant. The spectrum is reproduced by a Gaussian line shape plus a constant to mimic the Au continuum, times a Fermi-Dirac cutoff; the additional 10 meV experimental broadening is entirely negligible. The fit yields for Pb1 an energy width $\Delta E = 1.1 \pm 0.1$ eV (full width at half maximum, FWHM), which is anomalously large for a quasiparticle peak, but comparable to the width

of the corresponding Pb p_z band measured for a Pb ML on Ag(111).[7]

What is the origin of the anomalous momentum and energy broadening? Due to the Moiré modulation, the Pb atoms sit in inequivalent sites, and the energies of the Pb p orbitals, especially the energies of the p_z states which point towards the substrate, become site dependent. This effective disorder contributes to the spectral line widths, but quantitative simulations show that it cannot account for the large observed broadening.[7] A different, more effective broadening mechanism is triggered by the interaction between the Pb p_z orbitals and the Au surface state. The Au surface state extends further into the substrate than the overlayer p_z band. Through the hybridization with the surface state the p_z state can then more effectively couple with the Au bulk continuum of states, over a large range of k_z values that is inversely proportional to its (small) spatial extension in the z direction. For each value of the $k_{x,y}$ surface wave vector, the p_z state can essentially hybridize with the whole bulk continuum, thus acquiring an unusually large energy width. The large broadening is therefore the result of several factors: the nearly localized character of p_z yielding a large uncertainty on k_z; the good spatial overlap with the Au surface state; and the fact that the p_z band is entirely embedded in the bulk continuum.

Finally, we address the most striking aspect of the ARPES data, namely the different symmetries of the Fermi surface contours of the two p_{xy} derived bands of Fig. 2. Pb3 forms two sets of FS pockets, one for each rotational domain, around the corners ($\overline{\mathrm{K}}_{\mathrm{Pb}}$) of the Pb BZ, as expected for a band confined within the overlayer. By contrast, Pb2 forms a single hexagonal FS contour, aligned with the substrate BZ. How can two bands with the same origin exhibit such contrasting behavior? Fundamental principles require that all electronic states reflect the symmetry properties of the system, but such very general prescription cannot be strictly applied to our problem. The overall system has no clearly defined symmetry due to the coexisting incommensurate periodicities of overlayer and substrate. In similar circumstances, the simple notion of bands fades, and the relevant physical quantity is the spectral weight, which is distributed in energy and momentum space according to the strengths of the relevant interactions.[3] In this perspective, the data of Fig. 2 demonstrate a different degree of hybridization of the two p_{xy} bands with the substrate. The hybridization with Pb2 is stronger because this band is largely degenerate with the bulk continuum, namely near its Fermi surface crossing. Moreover, our TB results show that Pb2 hybridizes with Pb1, thus acquiring some p_z character, which also contributes to enhance the interaction of Pb2 with the substrate. The reduction of spectral intensity when Pb2 enters the continuum clearly indicates a sizable interaction. As a result, Pb2 strongly "feels" the potential of the substrate and conforms to its symmetry. Pb3, on the other hand, lies within the projected bulk band gap, and its interaction with the substrate is very weak. Therefore it remains confined within the overlayer and exhibits the symmetry of the two domains.

V. CONCLUSIONS

We have studied the structural and electronic properties of a Pb ML on Au(111) by STM and ARPES. We observed an incommensurate Moiré modulation, which is typical of Pb MLs on the (111) noble metal surfaces. We modeled the experimental band structure by a simple tight-binding model, which illustrates the importance of the overlayer-substrate interactions. The electronic structure of the interface is shaped by the different degrees of hybridization of the three Pb-derived p states. It varies from very strong (Pb1) to very weak (Pb3), and determines the energy-momentum spectral weight distribution, and the symmetry of the Fermi surface contours.

ACKNOWLEDGMENT

This work was supported by the Swiss NSF and by the MaNEP NCCR.

APPENDIX

The hybridization parameters used in the tight binding model presented in Fig. 4 are summarized in Table I.

TABLE I. Hybridization parameters following the notation of Ref. 26 in units of $(pp\sigma)$. Any proportional modification of all relevant parameters affects only the energy scaling.

Parameters	Fig. 4(a)	Fig. 4(b)	Fig. 4(c)
$(pp\sigma)$	1	1	1
$(pp\pi)$	0.3	0.3	0.3
$(ss\sigma)$	N/A	N/A	0.5
$(sp\sigma)$	N/A	N/A	0.5
z asymmetry	0	0.1	0

*alberto.crepaldi@epfl.ch

[1] A. Damascelli, Z. Hussain, and Z.-H. Shen, Rev. Mod. Phys. **75**, 473 (2003).

[2] M. Grioni, C. R. Ast, D. Pacilé, M. Papagno, H. Berger, and L. Perfetti, New J. Phys. **7**, 106 (2005).

[3] J. Voit, L. Perfetti, F. Zwick, H. Berger, G. Margaritondo, G. Grüner, H. Hochst, and M. Grioni, Science **290**, 501 (2000).

[4] J. Schäfer, E. Rotenberg, G. Meigs, S. D. Kevan, P. Blaha, and S. Hüfner, Phys. Rev. Lett. **83**, 2069 (1999).

[5] T. Yokoya, T. Kiss, A. Chainani, S. Shin, and K. Yamaya, Phys. Rev. B **71**, 140504 (2005).

[6] L. X. Yang, Y. Zhang, H. Ou, J. F. Zhao, D. Shen, B. Zhou, J. Wei, F. Chen, M. Xu, C. He *et al.*, Phys. Rev. Lett. **102**, 107002 (2009).

[7] C. R. Ast, D. Pacilé, M. Papagno, T. Gloor, F. Mila, S. Fedrigo, G. Wittich, K. Kern, H. Brune, and M. Grioni, Phys. Rev. B **73**, 245428 (2006).

[8] P. Moras, W. Theis, L. Ferrari, S. Gardonio, J. Fujii, K. Horn, and C. Carbone, Phys. Rev. Lett. **96**, 156401 (2006).

[9]T. Brugger, S. Günther, B. Wang, H. Dil, M.-L. Bocquet, J. Osterwalder, J. Wintterlin, and T. Greber, Phys. Rev. B **79**, 045407 (2009).
[10]M. Corso, W. Auwärter, M. Muntwiler, A. Tamai, T. Greber, and J. Osterwalder, Science **303**, 217 (2004).
[11]R. Laskowski, P. Blaha, T. Gallauner, and K. Schwarz, Phys. Rev. Lett. **98**, 106802 (2007).
[12]A. T. N'Diaye, S. Bleikamp, P. J. Feibelman, and T. Michely, Phys. Rev. Lett. **97**, 215501 (2006).
[13]S. Marchini, S. Günther, and J. Wintterlin, Phys. Rev. B **76**, 075429 (2007).
[14]T. Land, T. Michely, R. Behm, J. Hemminger, and G. Comsa, Surf. Sci. **264**, 261 (1992).
[15]I. Pletikosic, M. Kralj, P. Pervan, R. Brako, J. Coraux, A. T. N'Diaye, C. Busse, and T. Michely, Phys. Rev. Lett. **102**, 056808 (2009).
[16]S. Rusponi, M. Papagno, P. Moras, S. Vlaic, M. Etzkorn, P. M. Sheverdyaeva, D. Pacilé, H. Brune, and C. Carbone, Phys. Rev. Lett. **105**, 246803 (2010).
[17]N. Tsud, S. Fabik, V. Dudr, M. Vondracek, V. Chab, V. Matolin, and K. Prince, Surf. Sci. **542**, 112 (2003).
[18]F. Baumberger, A. Tamai, M. Muntwiler, T. Greber, and J. Osterwalder, Surf. Sci. **532–535**, 82 (2003).
[19]J. Camarero, J. Ferrón, V. Cros, L. Gómez, A. L. Vazquez de Parga, J. M. Gallego, J. E. Prieto, J. J. de Miguel, and R. Miranda, Phys. Rev. Lett. **81**, 850 (1998).
[20]F. Baumberger, W. Auwärter, T. Greber, and J. Osterwalder, Science **306**, 2221 (2004).
[21]S. Qin, J. Kim, Q. Niu, and C.-K. Shih, Science **324**, 1314 (2009).
[22]T. Zhang, P. Cheng, W.-J. Li, Y.-J. Sun, G. Wang, X.-G. Zhu, K. He, L. Wang, X. Ma, X. Chen *et al.*, Nat. Phys. **6**, 104 (2010).
[23]I. Horcas, R. Fernández, J. M. Gmez-Rodríguez, J. Colchero, J. Gmez-Herrero, and A. M. Baro, Rev. Sci. Instrum. **78**, 013705 (2007).
[24]T. Wiederholt, H. Brune, J. Wintterlin, R. Behm, and G. Ertl, Surf. Sci. **324**, 91 (1995).
[25]R. Mazzarello, A. D. Corso, and E. Tosatti, Surf. Sci. **602**, 893 (2008).
[26]J. C. Slater and G. F. Koster, Phys. Rev. **94**, 1498 (1954).
[27]L. Petersen and P. Hedegard, Surf. Sci. **459**, 49 (2000).
[28]M. Lindroos and A. Bansil, Phys. Rev. Lett. **77**, 2985 (1996).